

Quasi-periodic noise-like pulse mode locking in a fiber laser

Xinyu Hu(胡心语), Yuxuan Ren(任俞宣), Junsong Peng(彭俊松), Heping Zeng(曾和平)
Citation: Chin. Phys. B. 35, 094201 (2026). DOI: 10.1088/1674-1056/ae53b9 | CSTR: 32038.14.CPB.ae53b9
http://cpb.iphy.ac.cn; http://iopscience.iop.org/cpb

What follows is a list of articles you may be interested in

Comparison of cavity structures of 200 MHz repetition rate erbium-doped fiber lasers

Jiawei Liu(刘佳伟), Yuyao Zong(宗玉瑶), Yi Han(韩羿), Shiying Cao(曹士英)
Chin. Phys. B. 35, 064209 (2026). DOI: 10.1088/1674-1056/ae5f86 | CSTR: 32038.14.CPB.ae5f86

A 51-dB signal-to-noise ratio carrier-envelope offset frequency in an environmentally stabilized polarization-maintaining optical frequency comb

Yuyao Zong(宗玉瑶), Yi Han(韩羿), Jiawei Liu(刘佳伟), Cheng Ci(慈骋), Zhenyu Xue(薛振宇), Shiying Cao(曹士英)
Chin. Phys. B. 35, 064206 (2026). DOI: 10.1088/1674-1056/ae0924 | CSTR: 32038.14.CPB.ae0924

Generation of wavelength-tunable, bound-state and noise-like pulses in an all-polarization-maintaining laser ring cavity based on nonlinear polarization evolution

Yazhou Shi(石亚洲), Ze Li(李泽), Zhiguo Lv(吕志国)
Chin. Phys. B. 35, 054202 (2026). DOI: 10.1088/1674-1056/ae15f3 | CSTR: 32038.14.CPB.ae15f3

Dissipative soliton operation in a mode-locked laser based on thulium-doped fiber

Wen-Yan Zhang(张文艳), Lei Zheng(郑磊), Tian Zhang(张添), Nan-Nan Liu(刘楠楠), Li-Jie Geng(耿利杰), Kun Yang(杨坤), Li Zhan(詹黎)
Chin. Phys. B. 35, 044201 (2026). DOI: 10.1088/1674-1056/ae063c | CSTR: 32038.14.CPB.ae063c

Synchronized dual-wavelength mode-locked laser in normal dispersion regime

Yangrui Shi(史洋瑞), Haojing Zhang(张皓景), Yuxuan Ren(任俞宣), Junsong Peng(彭俊松), Heping Zeng(曾和平)
Chin. Phys. B. 34, 094207 (2025). DOI: 10.1088/1674-1056/add4fe | CSTR: 32038.14.CPB.add4fe

---

SPECIAL TOPIC — Nonlinear localized waves: Theory, methods and applications

Quasi-periodic noise-like pulse mode locking in a fiber laser

Xinyu Hu(胡心语)[1], Yuxuan Ren(任俞宣)[1], Junsong Peng(彭俊松)[1,2,3,†], and Heping Zeng(曾和平)[1,2,3,4,‡]

[1] *State Key Laboratory of Precision Spectroscopy, East China Normal University, Shanghai* 200062, *China*
[2] *Hainan Institute, East China Normal University, Sanya* 572024, *China*
[3] *Chongqing Institute, East China Normal University, Chongqing* 401120, *China*
[4] *Shanghai Research Center for Quantum Science, Shanghai* 200062, *China*

(Received 2 February 2026; revised manuscript received 13 March 2026; accepted manuscript online 18 March 2026)

Noise-like pulse (NLP) mode locking is generally thought to be stochastic. Here, we numerically find that NLP can exhibit quasi-periodicity, which can be controlled by the bandwidth of a spectral filter. The period can change from 250 to 2500 cavity round trips by tuning the bandwidth. Standard NLP without periodicity is also found by increasing the filter bandwidth.

Keywords: mode locking, laser, fiber, pulse

PACS: 42.55.Wd, 42.60.Fc, 42.65.Re, 42.65.Sf

DOI: 10.1088/1674-1056/ae53b9 **CSTR:** 32038.14.CPB.ae53b9

1. Introduction

Passively mode-locked fiber lasers that can emit ultrashort pulses have attracted considerable interest because of their low cost, compactness, and long-term stability. There are several coherent states in mode-locked lasers, including stationary[1–7] and breathing dissipative solitons.[8–13] These lasers can also generate incoherent states such as noise-like pulses (NLPs).[14] The NLP wave packet consists of many subpulses with random phase, amplitude, and duration. To date, NLP has been observed experimentally in fiber lasers operating in both the anomalous-dispersion[15–17] and normal-dispersion regimes.[18] NLP is believed to be stochastic, as recently demonstrated by the time-stretch technique,[19] which can measure the round-trip-resolved optical spectrum. Meanwhile, the time-lens technique, which can measure the round-trip-resolved temporal intensity of ultrashort pulses, also confirms the stochastic nature of NLP in the temporal domain.[20] Recent studies have revealed that mode-locked fiber lasers can support complex nonstationary pulse dynamics, including NLP transition states[21] and multicolor soliton switching.[22]

In this work, we numerically find that NLP can be quasiperiodic in a passively mode-locked fiber laser. Namely, NLP evolves with a period of a certain number of cavity round trips. Although the period is not sensitive to the gain saturation energy, we find that it is very sensitive to the bandwidth of the filter. An order-of-magnitude variation in the period is observed while the bandwidth is varied by only 2 nm. Such periodicity is lost when the bandwidth is further increased, resulting in standard NLP. A discrete mode-locked laser based on the generalized nonlinear Schrödinger equation (GNLSE) is employed to explore the NLP dynamics.

2. Numerical model

Figure 1 shows a schematic of the passively mode-locked fiber ring laser. The cavity consists of a wavelength-division multiplexer (WDM), a 2.5-m-long erbium-doped fiber (EDF), a Waveshaper that can be used to control both the dispersion and filter bandwidth of the laser, a saturable absorber (SA), a 4.7-m-long single-mode fiber (SMF), and an output coupler (OC) with a 90% coupling ratio. The intracavity pulse dynamics are simulated by solving the GNLSE using the split-step Fourier method[23]

$$\psi_z = -\frac{\mathrm{i}\beta_2}{2}\psi_{tt} + \mathrm{i}\gamma|\psi|^2\psi + \frac{g}{2}\left(\psi + \frac{1}{\Omega^2}\psi_{tt}\right). \tag{1}$$

Here, $\psi = \psi(z,t)$ denotes the slowly varying pulse envelope as a function of the propagation distance z and the retarded time t. β_2 is the group-velocity dispersion (GVD) parameter of the fiber. In the simulations, β_2 is set to 63.4 ps^2/km for the EDF and -23 ps^2/km for the SMF. γ is the Kerr nonlinearity coefficient, taken as 6.6 W$^{-1}\cdot$km^{-1} for the EDF and 1.65 W$^{-1}\cdot$km^{-1} for the SMF. The gain profile g is given by

$$g = \frac{g_0}{1 + E_\mathrm{p}/E_\mathrm{sat}}. \tag{2}$$

In this expression, $g_0 = 800$ km^{-1} is the small-signal gain of the EDF, $E_\mathrm{p} = \int \mathrm{d}t\,|\psi(z,t)|^2$ is the pulse energy and E_sat is the gain saturation energy, corresponding to the pump power in experiments. The gain is modeled with a parabolic spectral

†Corresponding author. E-mail: jspeng@lps.ecnu.edu.cn
‡Corresponding author. E-mail: hpzeng@phy.ecnu.edu.cn

© 2026 Chinese Physical Society and IOP Publishing Ltd. All rights, including for text and data mining, AI training, and similar technologies, are reserved.

profile of bandwidth $\Omega = 4.834$ THz (40 nm). Mode locking is implemented with SA whose transmission is given by

$$T = \sqrt{1 - q_0 - \frac{q_m}{1 + P(t)/P_{sat}}}, \tag{3}$$

where q_0 and q_m denote the SA nonsaturable loss and modulation depth, respectively. $P(t) = |\psi(z,t)|^2$ is the instantaneous pulse power, and P_{sat} is the saturation power of the SA. In the simulations, q_0, q_m, and P_{sat} are set to 0.4 W, 0.3 W, and 0.1 W, respectively.

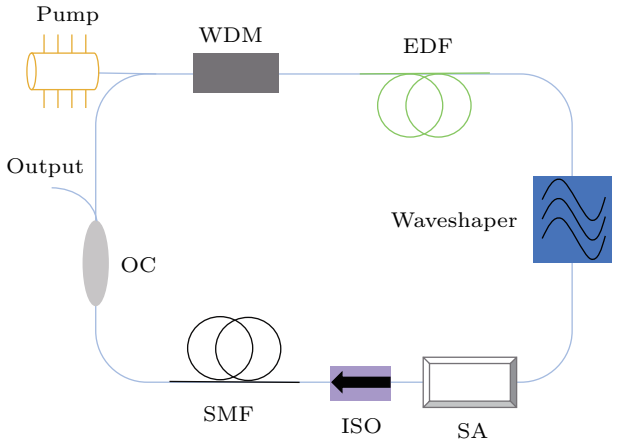


Fig. 1. Schematic of the passively mode-locked fiber ring laser. WDM, wavelength-division multiplexer; EDF, erbium-doped fiber; SA, saturable absorber; ISO, isolator; OC, optical coupler.

The key intracavity element is the Waveshaper, whose spectral response is described by[24]

$$H(\upsilon) = R(\upsilon)\exp\left[\frac{i\beta_{2,acc}(2\pi\upsilon)^2}{2}\right], \tag{4}$$

We use a Gaussian spectral profile $R(\upsilon) = \exp\left[-\upsilon^2/(2B^2)\right]$, where B denotes the filtering bandwidth. In the Waveshaper phase response, $\beta_{2,acc}$ (in ps^2) is the accumulated GVD. In the simulations, we set $\beta_{2,acc} = 0.4496$ ps^2. When $\beta_{2,acc} = 0$, the net dispersion is 0.0504 ps^2, corresponding to a weakly normal-dispersion regime. This dispersion contribution arises solely from the fiber components. In this laser, the net dispersion is determined by the lengths of EDF and SMF, as well as the accumulated GVD $\beta_{2,acc}$ imposed by the Waveshaper.

3. Results

The simulation starts from an initial chirp-free Gaussian pulse with a pulse width of 1 ps and peak power of 0.1 mW centered at 1575 nm. In the simulations, steady-state mode locking is achieved when the bandwidth of the filter is set to 10 nm and the gain saturation energy (E_{sat}) is 100 pJ. Figures 2(a) and 2(c) show the temporal and spectral evolution of the pulse over successive round trips (RTs). During propagation, the pulse maintains an invariant shape in both the time and frequency domains, suggesting a stable mode-locked state. Figures 2(b) and 2(d) present cross sections of the temporal and spectral profiles. The pulse has a duration of approximately 38 ps, a central wavelength of 1575 nm, and a spectral width of approximately 1.5 nm, indicating that the pulse is highly chirped.

With all the other parameters fixed, increasing E_{sat} to 400 pJ induces an erupting-type (ET) soliton explosion in the cavity.[25,26] As shown in Fig. 3(a), the dynamics remain in a single-pulse state throughout the entire process. However, during an explosion period, the pulse collapses into a fragmented structure characterized by multiple intensity dips, reminiscent shown in Fig. 3(c), the explosion is initiated by the progressive amplification of wings on its leading

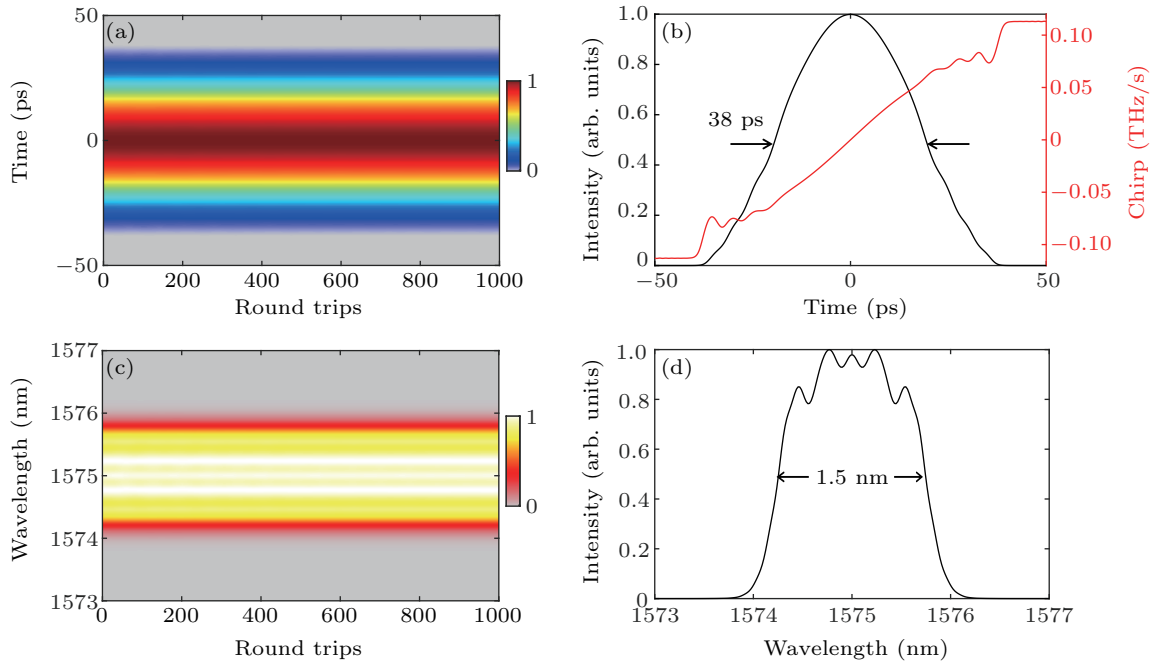


Fig. 2. Steady-state mode locking. (a) and (c) Temporal and spectral evolution of the pulse. (b) Temporal intensity profile of the pulse and the corresponding chirp. (d) Spectral intensity profile of the pulse.

of dark solitons. As edge, which subsequently merge into the main soliton. The merged state forms a temporally broadened pulse with a collapsed internal structure. Then the collapse vanishes, and the broad pulse relaxes to a smooth waveform and gradually narrows back to the pre-explosion soliton, accompanied by a forward shift of the pulse center. The corresponding spectral evolution is shown in Fig. 3(b). The soliton spectrum also collapses into a fragmented pattern during the explosion, and the spectrum in the collapsed stage is narrower than those before and after the event. Consistently, Fig. 3(d) shows that spectral narrowing coincides with an increase in the pulse energy during the ET soliton explosion.

As indicated in Figs. 3(e) and 3(g), the pulse shape remains nearly unchanged before and after the explosion, except for a shift in the pulse center. In contrast, during the explosion, the temporal profile is broken by multiple dips. Such ET soliton explosions can lead to timing jitter in practical mode-locked fiber lasers. Notably, this jitter is not caused by external perturbations but originates from the intrinsic nonlinear dynamics of dissipative solitons. Furthermore, Figs. 3(f) and 3(h) show that the spectrum undergoes a similar collapse, closely resembling the collapsed spectra reported experimentally during soliton explosions.[27] Additionally, the leading and trailing edges in Fig. 3(e) exhibit small ripples, which manifest in the spectrum as localized oscillatory features near the spectral center, as highlighted in the inset of Fig. 3(f).

With all the other parameters fixed, further increasing E_{sat} to 2000 pJ leads to the generation of a quasi-periodic NLP state in the cavity. As shown in Fig. 4(a), the quasi-periodic NLP has a period of approximately 500 round trips. The period is determined from the peak-to-peak spacing of the pulse-energy sequence over successive cavity round trips, where the pulse energy at each round trip is calculated from the simulated pulse profile. This estimate is consistent with the energy evolution represented by the black trace. Figure 4(b) shows the corresponding spectral evolution, which also exhibits strong fluctuations. To reveal more details of the NLP dynamics, representative temporal profiles at RT = 571 and RT = 663 are shown in Fig. 4(c). The pulse at RT = 571 shows a pronounced protrusion on its leading-edge envelope, whereas the pulse at RT = 663 exhibits a similar protrusion on its trailing-edge envelope. The corresponding spectra at these round trips are shown in Fig. 4(d).

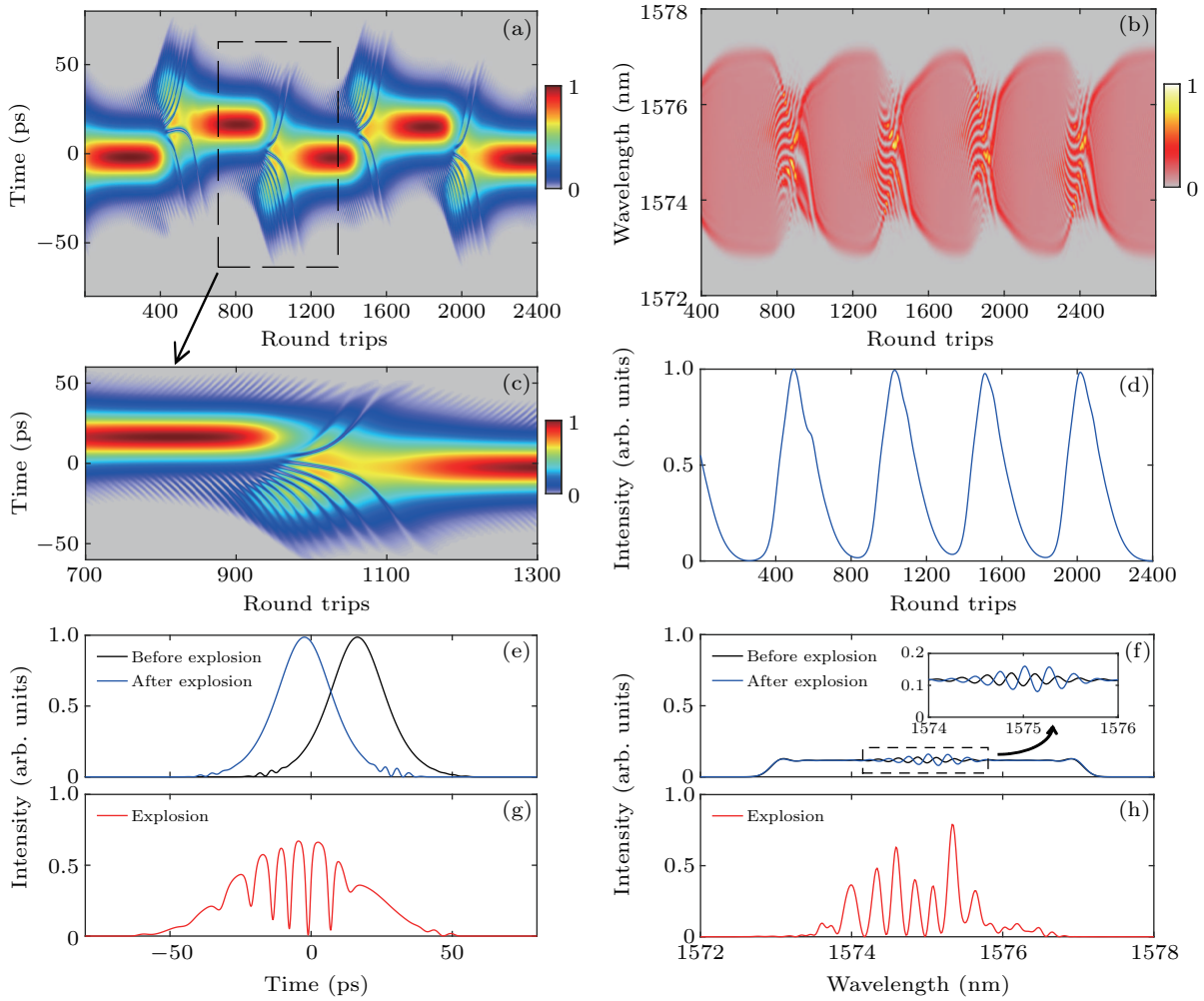


Fig. 3. Evolution of erupting-type soliton explosion. (a) Temporal evolution of the pulse. (b) Spectral evolution of the pulse. (c) Temporal evolution over one explosion period. (d) Pulse-energy evolution. (e) and (g) Temporal profiles at three representative stages within one explosion period. (f) and (h) Corresponding spectra at the three stages.

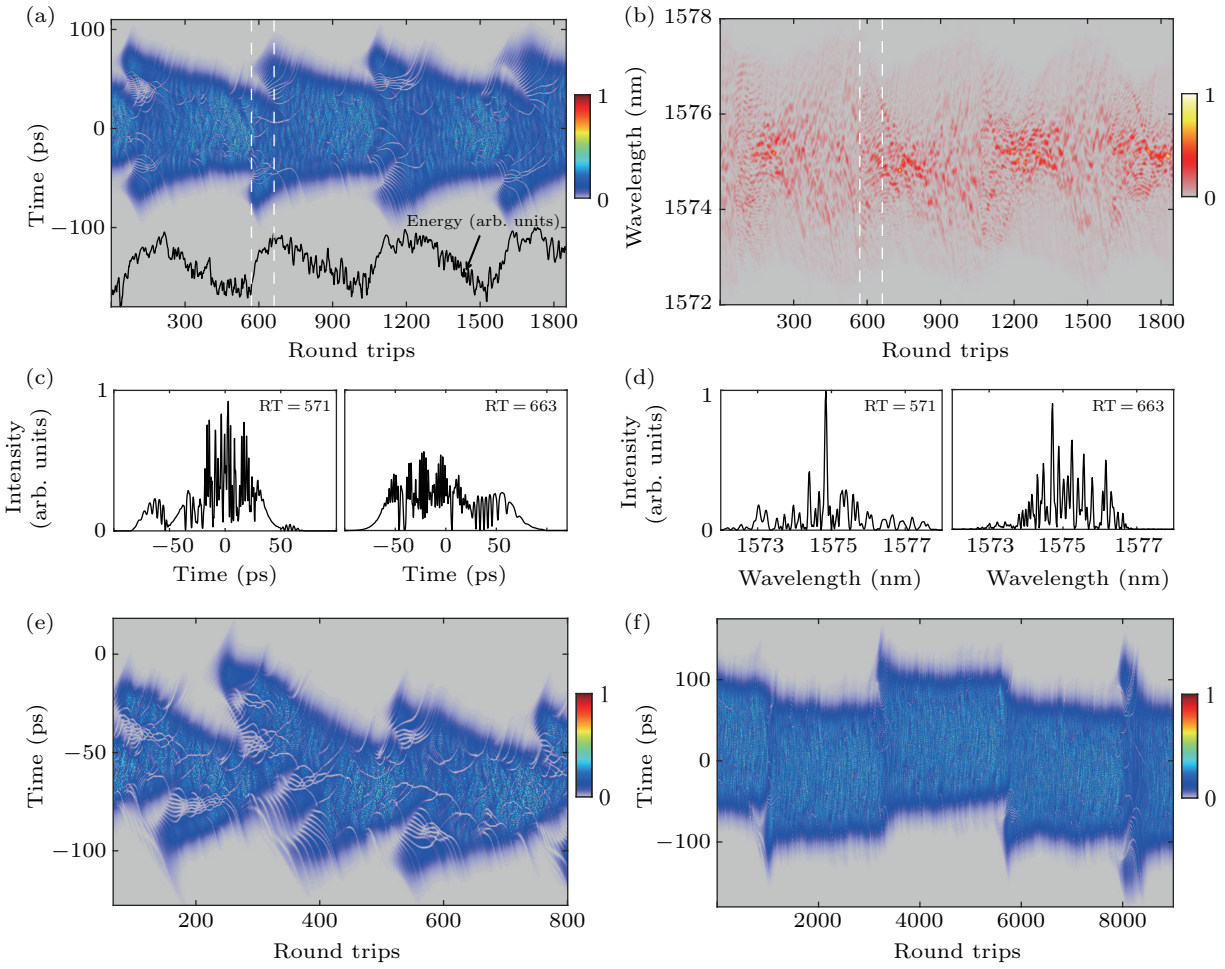


Fig. 4. Periodic NLP dynamics. (a) and (b) Temporal and spectral evolution at a Waveshaper bandwidth of 10 nm. (c) and (d) Temporal and corresponding spectral profiles at round trips 571 and 663. (e) Temporal evolution at a Waveshaper bandwidth of 8 nm. (f) Temporal evolution at a Waveshaper bandwidth of 12 nm.

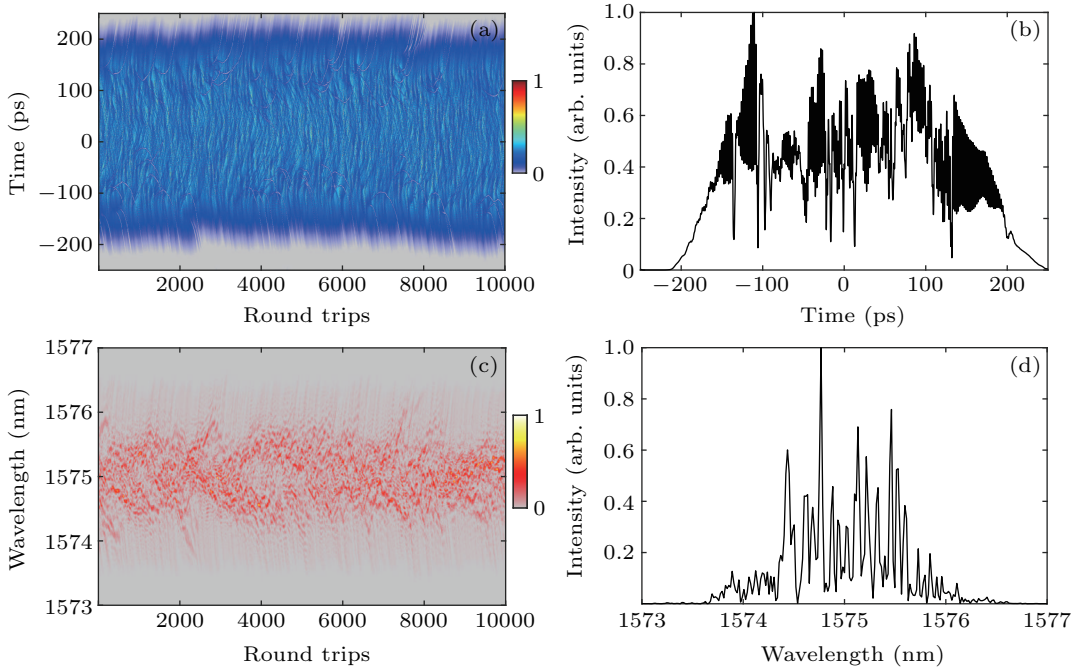


Fig. 5. Standard NLP state without periodicity. (a) and (c) Respective temporal and spectral evolution of the NLP when the filter bandwidth is increased to 18 nm. (b) and (d) Respective temporal and spectral intensity profiles.

It is natural to ask whether the period can be varied by tuning the gain saturation energy (E_{sat}). However, we find that varying E_{sat} has a negligible effect on the NLP period. In contrast, changing the filter bandwidth yields a pronounced variation. Figures 4(e) and 4(f) present results obtained at the same $E_{\text{sat}} = 2000$ pJ, but with different bandwidths of 8 nm and 12 nm, yielding periods of 250 and 2500 round trips, respectively.

With a filter bandwidth of 18 nm and a gain saturation energy of 2000 pJ, the observed quasi-periodic behavior disappears, giving rise to standard NLP. Figures 5(a) and 5(c) show the temporal and spectral evolution over successive round trips. In contrast to the clearly quasi-periodic dynamics in Fig. 4(a), the pulse exhibits a conventional NLP state without periodicity. Figures 5(b) and 5(d) provide cross sections of the temporal and spectral evolution, showing a relatively broad temporal width of approximately 300 ps and a fluctuating optical spectrum.

4. Conclusion

In conclusion, we systematically study the NLP dynamics in a mode-locked fiber laser. Increasing the gain saturation energy solely drives the system from a stable dissipative soliton, to an eruptive soliton explosion, and finally to a quasi-periodic NLP state. Distinct from the conventional regimes, the quasi-periodic NLP obtained under strong spectral filtering is characterized by a distinct period. Its periodicity can be tuned by adjusting the filter bandwidth. These results may bring new insights into the study of non-equilibrium processes in fiber lasers. Furthermore, this work clearly demonstrates that spectral filtering can serve as an additional degree of freedom for exploring novel soliton dynamics.

Acknowledgments

Project supported by the Innovation Program for Quantum Science and Technology (Grant No. 2023ZD0301000), the National Natural Science Fund of China (Grant Nos. 12434018, 62475073, 1243000542, 11621404, 11561121003, 11727812, 61775059, 12074122, 62405090, 62035005, and 11704123), the Shanghai Natural Science Foundation (Grant No. 23ZR1419000), and the China Postdoctoral Science Foundation (Grant Nos. 2023M741188 and 2024T170275).

References

[1] Kelly S M J 1992 *Electron. Lett.* **28** 806
[2] Tamura K, Ippen E P, Haus H A and Nelson L E 1993 *Opt. Lett.* **18** 1080
[3] Ilday F Ö, Buckley J R, Clark W G and Wise F W 2004 *Phys. Rev. Lett.* **92** 213902
[4] Chong A, Buckley J, Renninger W and Wise F 2006 *Opt. Express* **14** 10095
[5] Chang W, Ankiewicz A, Soto-Crespo J M and Akhmediev N 2008 *Phys. Rev. A* **78** 023830
[6] Ding E, Grelu P and Kutz J N 2011 *Opt. Lett.* **36** 1146
[7] Turitsyn S K, Bale B G and Fedoruk M P 2012 *Phys. Rep.* **521** 135
[8] Peng J, Boscolo S, Zhao Z and Zeng H 2019 *Sci. Adv.* **5** eaax1110
[9] Wu X, Zhang Y, Peng J, Boscolo S, Finot C and Zeng H 2022 *Nat. Commun.* **13** 5784
[10] Wu X, Peng J, Boscolo S, Finot C and Zeng H 2023 *Phys. Rev. Lett.* **131** 263802
[11] Kang H, Zhou A, Zhang Y, Wu X, Yuan B, Peng J, Finot C, Boscolo S and Zeng H 2024 *Phys. Rev. Lett.* **133** 263801
[12] Wu X, Peng J, Yuan B, Boscolo S, Finot C and Zeng H 2025 *Sci. Adv.* **11** eads3660
[13] Peng J, Wu X, Kang H, Zhou A, Zhang Y, Zeng H, Finot C and Boscolo S 2025 *Adv. Phys. X* **10** 2580628
[14] Horowitz M, Barad Y and Silberberg Y 1997 *Opt. Lett.* **22** 799
[15] Tang D Y, Zhao L M and Zhao B 2005 *Opt. Express* **13** 2289
[16] Zhao L M and Tang D Y 2006 *Appl. Phys. B* **83** 553
[17] Liu S, Yan F, Li Y, Zhang L, Bai Z, Zhou H and Hou Y 2016 *Photonics Res.* **4** 318
[18] Zhao L M, Tang D Y, Wu J, Fu X Q and Wen S C 2007 *Opt. Express* **15** 2145
[19] Runge A F J, Aguergaray C, Broderick N G R and Erkintalo M 2013 *Opt. Lett.* **38** 4327
[20] Meng F, Lapre C, Billet C, Sylvestre T, Merolla J M, Finot C, Turitsyn S K, Genty G and Dudley J M 2021 *Nat. Commun.* **12** 5567
[21] Si Z Z, Ju Z T, Ren L F, Wang X P, Malomed B A and Dai C Q 2025 *Laser Photon. Rev.* **19** e2401019
[22] Jia Y H, Si Z Z, Ju Z T, Feng H Y, Zhang J H, Yan X and Dai C Q 2025 *Sci. China Phys. Mech. Astron.* **68** 284211
[23] Haus H A 2000 *IEEE J. Sel. Top. Quantum Electron.* **6** 1173
[24] Boscolo S, Finot C, Karakuzu H and Petropoulos P 2014 *Opt. Lett.* **39** 438
[25] Soto-Crespo J M, Akhmediev N and Ankiewicz A 2000 *Phys. Rev. Lett.* **85** 2937
[26] Akhmediev N and Soto-Crespo J M 2003 *Phys. Lett. A* **317** 287
[27] Liu M, Luo A, Yan Y, Hu S, Liu Y, Cui H, Luo Z and Xu W 2016 *Opt. Lett.* **41** 1181